

Locational Pricing for Generative-AI Services via Token-Flow Market Clearing

Shaohui Liu

Massachusetts Institute of Technology
Cambridge, Massachusetts, USA
shaohuil@mit.edu

Abstract

GenAI services are in an early yet fast expanding phase. Providers compete on model capability and service quality, while the underlying infrastructure remains expensive and heterogeneous across regions, workloads, and compute assets. If these services diffuse into routine daily use, the relevant engineering problem becomes not only better models but also efficient dispatch on a geographically distributed AI service infrastructure. To address this, we formulate a network-constrained token-flow market that clears AI workloads across compute nodes and communication links. The baseline model is a linear program that co-optimizes routing and processing subject to compute-capacity and bandwidth constraints; its dual variables define location- and workload-specific marginal service prices. We further introduce a transfer-aware extension that prices data movement in physical units and isolates bandwidth congestion rents. In a 5-node U.S. case study, the transfer-aware model uncovers four saturated backbone links and raises total operating cost by 2.7% relative to the token-equivalent baseline, while tightening the chatbot latency limit from 100 ms to 15 ms increases one locational price by 117%. A 20-node scale-up exhibits the same merit-order dispatch logic and becomes infeasible once demand exceeds aggregate capacity. These results suggest that locational pricing is a useful organizing principle for operating an emerging AI service infrastructure and, over time, for designing competitive markets around it.

Keywords

generative AI, AI service infrastructure, data centers, network flow, token market, locational marginal pricing

1 Introduction

Generative-AI (GenAI) services are still in an early but fast-growing stage. Recent indicators point to rapid expansion. The 2025 Stanford AI Index reports that global private investment in generative AI reached \$33.9 billion in 2024 and that organizational use of generative AI in at least one business function rose from 33% to 71% year over year [19]. Deloitte’s latest enterprise survey likewise finds AI deployment moving from pilot programs toward broader organizational rollout [7]. Service prices remain high for routine use, while providers compete primarily on model capability and quality of service. Additionally, infrastructure deployment is driven more by frontier performance than by transparent cost recovery. While that posture is natural in an immature sector, it is unlikely to be

the end state. When GenAI becomes a routine input to daily work and consumption, the market scale will grow substantially and the economics of operating the underlying infrastructure will become as important as the models themselves.

In that regime, the relevant physical system is not a single cluster but a geographically distributed collection of data centers, backbone links, and service endpoints. To avoid the ambiguity of “AI network,” we refer to this coupled system as *distributed AI service infrastructure*. A user request may be served by one of many candidate sites, and the marginal cost of serving that request depends jointly on local compute availability, electricity price, network transfer cost, and latency. This makes the allocation of AI workloads a network-constrained resource-allocation problem rather than a purely local server-scheduling problem.

Heterogeneity is central rather than incidental. Workload classes differ in latency tolerance, data volume per million tokens, and energy intensity, while compute assets differ in accelerator type, vintage, efficiency, and cost. As a result, hardware that is no longer cost-effective for frontier interactive services can still remain economically valuable for lower-priority, batch, or less latency-sensitive workloads. A credible market design therefore should not assume a homogeneous fleet. It should price a diversified asset base and reveal when older or cheaper resources remain the efficient marginal supplier.

This observation matters for both operations and market design. Electricity is already a major component of data-center operating expenditure, often on the order of 20–40% of total cost [8, 11], while public initiatives on compute interconnection increasingly treat distributed compute as an infrastructure resource that should be shared and scheduled across regions [9, 14, 15]. Yet most current API pricing remains largely location-agnostic, even though the underlying physical system is strongly location dependent. The analogy to electricity markets should not be overstated, but the historical lesson is relevant: once a networked service becomes critical infrastructure, efficient dispatch and transparent locational pricing become increasingly important. We do not claim that today’s GenAI sector already operates as such a market. Rather, we study the pricing objects and clearing rules that become relevant as the sector matures toward one.

To this end, this paper proposes a market-clearing abstraction for that setting. We model GenAI service provision on distributed AI service infrastructure as a *token-flow network* in which user demand is routed across communication links and processed at compute nodes. The resulting optimization resembles minimum-cost flow, but the economic interpretation is closer to locational marginal pricing in electricity markets, where dual variables on the



This work is licensed under a Creative Commons Attribution-NonCommercial-NoDerivatives 4.0 International License.

nodal balance constraints become location- and workload-specific marginal service prices.

1.1 Background and relation to prior work

The paper connects three mature modeling templates. Electricity markets show how a centrally cleared, network-constrained dispatch problem can produce locational prices. Transportation and logistics show how commodities can be routed through capacitated networks. Communication-network pricing shows how link shadow prices can be interpreted as congestion signals. Our contribution is to adapt these ideas to GenAI service tokens, where compute, transfer, and latency are all workload dependent.

In power systems, optimal power flow and locational marginal pricing combine nodal balance, generator limits, and line constraints to obtain prices that decompose into energy and congestion components [2, 5, 10]. We inherit the use of balance-constraint dual variables as marginal prices, but our nodes are compute locations rather than buses, and the scarce local resource is class-specific AI serving capacity rather than generation output.

Minimum-cost and multicommodity-flow models provide the mathematical backbone for routing multiple commodities over shared capacities [1, 3, 4, 18]. The token-flow program is deliberately close to this family. The difference is not the algorithmic structure, but the commodity definition: useful GenAI tokens carry class-specific energy intensity, data volume per million tokens, latency eligibility, and settlement interpretation.

Communication-network congestion control and network utility maximization provide a complementary view in which link prices decentralize rate-allocation decisions [12, 13, 16]. Those models usually price communication capacity itself. Here communication is only one layer of the service: routing a request also consumes scarce compute at the destination, so the economically relevant price must include both transfer scarcity and compute scarcity.

Finally, the cloud and AI-infrastructure context motivates why these pricing objects matter now. Data-center operating cost, public compute interconnection initiatives, and AI-service metering all point toward a more infrastructure-like service layer [8, 9, 14]. The novelty claimed here is therefore the identification of the economically relevant commodity, constraints, and dual prices for geographically distributed GenAI service infrastructure than a new flow algorithm.

Contributions. Our contributions are threefold.

- We formulate a linear market clearing model for GenAI services that jointly route and process requests under compute-capacity and bandwidth constraints on a geographically distributed and heterogeneous infrastructure.
- We derive the associated locational marginal service prices and show how they decompose into energy cost, compute scarcity rent, routing cost, and link congestion rent. We also introduce a transfer-aware extension that prices network usage in physical data units (GB/s).
- On 5-node and 20-node U.S. data-center networks, the case studies show merit-order dispatch, scarcity transitions in image generation, transfer bottlenecks hidden by token-equivalent bandwidth models, and strong regional price separation under tight latency constraints.

The rest of the paper is organized as follows. Section 2 presents the token-flow market model and its price interpretation. Section 3 describes the data sources, scenario construction, and calibration choices. Section 4 reports the numerical results, and Sections 5 and 6 discuss limitations and summarize the paper.

2 Token-Flow Market Model

2.1 System abstraction

Let \mathcal{N} be the set of compute nodes and $\mathcal{E} \subseteq \mathcal{N} \times \mathcal{N}$ the directed communication network. Workloads are partitioned into job classes $k \in \mathcal{K}$, such as interactive chat, image generation, code review, and batch training. For each class k , demand $d_{j,k}$ denotes the useful token rate requested at node j . Operationally, $d_{j,k}$ is an exogenous request-arrival rate at origin region j . The market clearing problem decides whether that demand is processed locally or routed to another compute node subject to constraints. The injection pattern is therefore an input to the market, and changing the demand vector can change both dispatch and prices.

We use two decision variables for each class k :

- $f_{i,j,k} \geq 0$: token flow of class k routed on arc (i, j) ;
- $x_{j,k} \geq 0$: token rate of class k processed at node j .

Each node j has class-specific processing capacity $C_{j,k}$, local electricity price p_j^{elec} (\$/kWh), and class-specific energy requirement $e_{j,k}$ (kWh/M tokens). The resulting marginal processing cost is

$$g_{j,k} := p_j^{\text{elec}} e_{j,k} \quad (\$/M \text{ tokens}).$$

Each arc (i, j) has token-equivalent capacity B_{ij} and routing cost $c_{ij,k}$, which captures latency penalties, network charges, or other per-token delivery costs in the baseline model. For latency-sensitive workloads we restrict routing to a feasible arc set $\mathcal{E}_k \subseteq \mathcal{E}$ defined by a class-specific latency rule. In the numerical study, this rule is implemented by removing arcs whose latency exceeds the class-specific threshold.

2.2 Baseline market-clearing program

Let $\mathbf{A} \in \{-1, 0, 1\}^{|\mathcal{N}| \times |\mathcal{E}|}$ be the node-arc incidence matrix, with $+1$ at the sending node and -1 at the receiving node for each arc, so that $\mathbf{A}\mathbf{f}_k$ is net outbound flow. For each class k , let $\mathbf{f}_k \in \mathbb{R}_+^{|\mathcal{E}|}$ collect arc flows, $\mathbf{x}_k, \mathbf{d}_k, \mathbf{g}_k, \mathbf{C}_k \in \mathbb{R}_+^{|\mathcal{N}|}$ collect node variables and parameters, and let \mathbf{B} denote the vector of token-equivalent arc capacities. The baseline clearing problem is formulated as the following linear program:

$$\min_{\{\mathbf{f}_k, \mathbf{x}_k\}_{k \in \mathcal{K}}} \sum_{k \in \mathcal{K}} (\mathbf{c}_k^\top \mathbf{f}_k + \mathbf{g}_k^\top \mathbf{x}_k) \quad (1a)$$

$$\text{s.t. } \mathbf{A}\mathbf{f}_k + \mathbf{x}_k = \mathbf{d}_k, \quad \forall k \in \mathcal{K}, \quad (1b)$$

$$\mathbf{0} \leq \mathbf{x}_k \leq \mathbf{C}_k, \quad \forall k \in \mathcal{K}, \quad (1c)$$

$$\sum_{k \in \mathcal{K}} \mathbf{f}_k \leq \mathbf{B}, \quad (1d)$$

$$\mathbf{f}_k \geq \mathbf{0}, \quad \forall k \in \mathcal{K}. \quad (1e)$$

where (1b) enforces flow conservation where all demand must either be processed locally or routed elsewhere for service. Constraint (1c) imposes node-level compute limits, and (1d) captures shared communication capacity. The objective minimizes operating cost while serving all demand.

In scalar form, the balance equation is $\sum_h f_{jh,k} + x_{j,k} = d_{j,k} + \sum_i f_{ij,k}$: origin demand and inbound traffic must be either processed at node j or sent onward. The routing coefficient can be written as $c_{ij,k} = c_{ij,k}^{\text{route}} + w_{ij}a_k$, where w_{ij} is a transfer tariff in \$/GB and a_k is the payload size of a useful token. The baseline token-equivalent bandwidth approximation sets $B_{ij} = W_{ij}/a$, with $a = \min_{k \in \mathcal{K}} a_k$; this keeps the LP compact but is optimistic for data-heavy classes. Latency requirements are enforced by setting $f_{ij,k} = 0$ when $\tau_{ij} > L_k^{\text{max}}$. Taken together, the equations define a linear clearing problem in which electricity cost sets the merit order, node capacity creates compute scarcity, and link limits create network scarcity.

The equality in (1b) is a must-serve abstraction. This is appropriate for a first market-clearing model under a service-obligation interpretation, but production systems can queue, degrade, or drop requests. A partial-service extension would introduce unmet demand $y_{j,k} \geq 0$ and penalty $\rho_{j,k}$, replace the balance with $Af_k + x_k + y_k = d_k$, and add $\sum_{j,k} \rho_{j,k} y_{j,k}$ to the objective. That extension converts infeasibility into deferred or shed service and caps scarcity prices at the value of lost service.

Remark (Economic-Dispatch Benchmark). A simpler benchmark would clear demand against node-level marginal processing costs and capacities without explicit network constraints, in the spirit of economic dispatch in power systems [17, 20]. We use the network-constrained model as the main object because transfer and latency are not secondary refinements for GenAI services, as they materially affect both dispatch and prices. Section 4 therefore compares nested formulations of the same clearing abstraction rather than unrelated cloud schedulers.

2.3 Dual prices and economic interpretation

Let π_k be the dual multipliers on the nodal balance constraints (1b), $\mu_k \geq 0$ the multipliers on the compute-capacity upper bounds (1c), and $\eta \geq 0$ the multipliers on the link-capacity constraints (1d). Using the sign convention that π_k measures the marginal cost of one additional unit of demand, the Lagrangian of (1) is

$$\mathcal{L} = \sum_{k \in \mathcal{K}} \left[c_k^\top f_k + g_k^\top x_k - \pi_k^\top (Af_k + x_k - d_k) + \mu_k^\top (x_k - C_k) \right] + \eta^\top \left(\sum_{k \in \mathcal{K}} f_k - B \right). \quad (2)$$

Minimizing (2) over the nonnegative primal variables produces the dual feasibility conditions

$$A^\top \pi_k \leq c_k + \eta, \quad \forall k \in \mathcal{K}, \quad (3)$$

$$\pi_k \leq g_k + \mu_k, \quad \forall k \in \mathcal{K}. \quad (4)$$

and the KKT relations

$$0 \leq c_k + \eta - A^\top \pi_k \perp f_k \geq 0, \quad (5)$$

$$0 \leq g_k + \mu_k - \pi_k \perp x_k \geq 0. \quad (6)$$

The multiplier $\pi_{j,k}$ is the marginal system cost of serving one additional token of class k at node j , i.e., the *locational marginal service price*. Complementary slackness gives two key identities.

For any active arc (i, j) used by class k ,

$$\pi_{i,k} - \pi_{j,k} = c_{ij,k} + \eta_{ij}^*. \quad (7)$$

Hence the price difference across a used link equals private routing cost plus a congestion rent if the link is scarce.

For any active processing decision at node j ,

$$\pi_{j,k}^* = g_{j,k} + \mu_{j,k}^* = p_j^{\text{elec}} e_{j,k} + \mu_{j,k}^*. \quad (8)$$

Thus the local service price decomposes into marginal energy cost plus a compute-scarcity rent. If node j has spare class- k capacity, then $\mu_{j,k}^* = 0$.

Combining (7) and (8) along an active path $P(o, s)$ from origin o to serving node s yields

$$\pi_{o,k}^* = g_{s,k} + \mu_{s,k}^* + \sum_{(i,j) \in P(o,s)} (c_{ij,k} + \eta_{ij}^*). \quad (9)$$

Equation (9) is the central pricing result of the paper: token prices inherit the same energy-plus-congestion logic that underlies electricity LMPs, but with an additional compute-scarcity term that is specific to AI infrastructure.

2.4 Transfer-aware extension and settlement

The baseline model measures bandwidth in token-equivalent units. That is insufficient when workload classes induce very different data volumes per useful token. Let $\gamma_{ij,k}$ denote the effective data requirement (GB/token) of serving one useful token of class k on arc (i, j) after protocol overhead, let w_{ij} be the exogenous transfer tariff (\$/GB), and let W_{ij} be the physical link capacity (GB/s). The transfer-aware refinement becomes

$$\min_{\{f_k, x_k\}_{k \in \mathcal{K}}} \sum_{k \in \mathcal{K}} ((c_k^{\text{route}})^\top f_k + g_k^\top x_k + w^\top \Gamma_k f_k) \quad (10a)$$

$$\text{s.t. } Af_k + x_k = d_k, \quad \forall k \in \mathcal{K}, \quad (10b)$$

$$0 \leq x_k \leq C_k, \quad \forall k \in \mathcal{K}, \quad (10c)$$

$$\sum_{k \in \mathcal{K}} \Gamma_k f_k \leq W, \quad (10d)$$

$$f_k \geq 0, \quad \forall k \in \mathcal{K}, \quad (10e)$$

where $\Gamma_k := \text{diag}(\gamma_{ij,k})$ over arcs $(i, j) \in \mathcal{E}$.

For any active transfer arc, the dual relation becomes

$$\pi_{i,k}^* - \pi_{j,k}^* = c_{ij,k}^{\text{route}} + \gamma_{ij,k} (w_{ij} + \eta_{ij}^*). \quad (11)$$

This version isolates physical-network payments and gives the congestion rent units of \$/GB instead of \$/token.

The same dual variables define an economically consistent settlement rule. Demand at node j pays $\pi_{j,k}^* d_{j,k}$, compute providers receive $(g_{j,k} + \mu_{j,k}^*) x_{j,k}^*$, and network providers receive $(w_{ij} + \eta_{ij}^*) q_{ij,k}$ on carried traffic $q_{ij,k} = \gamma_{ij,k} f_{ij,k}$. Any residual is a merchandising surplus analogous to congestion revenue in electricity markets.

3 Experimental Setup

For case studies we aim to evaluate three questions: (i) what dispatch and price patterns emerge in the baseline token-flow market, (ii) how scarcity and congestion evolve as demand grows, and (iii) how transfer-aware and latency-aware variants change the market outcome.

All experiments are generated with the `TokenFlowMarket.jl` artifact¹, implemented in JuMP with Gurobi as the default LP/QP

¹Code and examples available at <https://github.com/ShaohuiLiu/TokenFlowMarket.git>.

Table 1: Five-node testbed used for the case study.

Site	Power (MW)	Elec. price (\$/kWh)
Ashburn/NoVA	2000	0.078
Dallas/Fort Worth	1200	0.072
Silicon Valley	800	0.180
Chicago	1000	0.085
Seattle/Quincy	600	0.052

solver and with explicit dual extraction for nodal prices, link congestion rents, and compute scarcity rents. The primary dataset is a 20-hub U.S. registry compiled from Data Center Map and manually curated into a table containing hub identifier, metro name, state, latitude, longitude, facility count, and estimated site power (MW) [6]. State-level electricity prices are taken from 2025 EIA industrial retail rates and joined by state [21]. The 5-node testbed is the subset Ashburn/NoVA, Dallas/Fort Worth, Silicon Valley, Chicago, and Seattle/Quincy; the 20-node experiment uses the full registry.

Scenario construction follows the package’s public data pipeline. First, estimated site power is converted into synthetic class-specific processing capacities using fixed throughput-per-MW coefficients: 5000 chatbot tokens/s/MW, 200 image tokens/s/MW, 4000 code-review tokens/s/MW, and 1000 batch-training tokens/s/MW. Second, bidirectional arcs are created between hubs within 2500 km, while a synthetic tier-1 backbone connects the major metros Ashburn, Dallas, Silicon Valley, Chicago, Atlanta, and New York at 100 Gbps; all other links use 10 Gbps. Link latency is approximated as fiber propagation plus a 5 ms per-hop overhead, $\tau_{ij} = \text{dist}_{ij}/200 + 5$, and the transfer tariff is fixed at \$0.01/GB. Third, demand is generated from state-level population weights and base per-class rates of 50,000 chatbot, 5,000 image-generation, 30,000 code-review, and 10,000 batch-training tokens/s at weight 1.0. The primary operating point uses demand scale 35 \times , which yields 16.29 million tokens/s of aggregate demand and places the system in an economically interesting interior regime with both compute scarcity and network congestion. We also report a 20-node U.S. scale-up to test whether the same qualitative patterns persist in a larger network.

Note that these throughput, energy, and transfer-volume coefficients are stylized scenario parameters rather than measurements from a particular provider. They are chosen to separate workload classes by plausible orders of magnitude, where image generation is compute- and transfer-heavy, chat is latency-sensitive and data-light, and batch work is more delay tolerant. The precise scarcity thresholds should therefore be read as scenario outcomes, while the qualitative mechanisms rely on relative heterogeneity. While we hold explicit throughput and transfer-volume sensitivity for future work, the present paper reports demand, latency, and electricity-price sweeps.

Table 2 summarizes the four typical workload classes using per-million-token units for readability. They differ by more than two orders of magnitude in energy intensity and by roughly five orders of magnitude in data volume, which is precisely why pricing compute and transfer jointly is important.

Table 2: Workload classes used in the case study in per million useful tokens.

Class	GB/M tokens	kWh/M tokens	Latency bound
Interactive chat	0.5	1	100 ms
Image generation	100	500	unconstrained
Code review	1	2	200 ms
Batch training	10	10	unconstrained

Table 3: Selected locational price decompositions at the 5-node baseline operating point reported in \$/M tokens where LMP = Energy cost + Scarcity charge.

Node	Class	LMP	Energy	Scarcity
Ashburn	Chat	0.078	0.078	0
Dallas	Chat	0.078	0.072	0.006
Dallas	Image	41.50	36.00	5.50
Seattle	Image	41.47	26.00	15.47
Seattle	Batch	0.694	0.520	0.174

4 Numerical Results

4.1 Baseline dispatch follows locational cost and capacity scarcity

Figure 2 combines a geographic and algebraic view of the 5-node baseline clearing outcome at the primary operating point. The key dispatch pattern is in merit-order that lower-cost nodes absorb most of the workload, while the most expensive node is displaced. Dallas and Seattle serve as the primary workhorses, whereas Silicon Valley is completely priced out despite nontrivial installed capacity. The result shows direct implication of nodal prices being anchored to the cheapest feasible marginal supplier.

The pricing decomposition confirms that scarcity rents are concentrated in the classes and locations where capacity binds. Table 3 reports selected node–class pairs, not the full site list. Chicago carries image-generation volume in Figure 2, and Silicon Valley is part of the network but is displaced at this operating point. Seattle’s image-generation price is especially revealing: only \$26.00/M tokens comes from energy, while \$15.47/M tokens, or 37.3% of the total price, comes from compute scarcity. By contrast, Ashburn’s chatbot price is entirely explained by energy cost because the corresponding capacity is slack.

Note that one subtle but important implication is that a node’s local energy cost does not by itself determine its price. Silicon Valley’s chatbot energy cost is \$0.18/M tokens, but because no chatbot demand is served there in the baseline optimum, the local nodal price is instead pinned down by the cheapest feasible external supply chain. In other words, locational marginal prices are system-level marginal values, not local average costs.

4.2 Sharp scarcity transition from demand growth

Next we sweep the demand scale from 1 \times to 45 \times , as in Figure 3, and two features stand out. First, mean chatbot prices are relatively stable because chatbot capacity remains abundant over most of the range. Second, image generation exhibits a pronounced scarcity cliff. Between scale 35 \times and 40 \times , the mean image-generation price

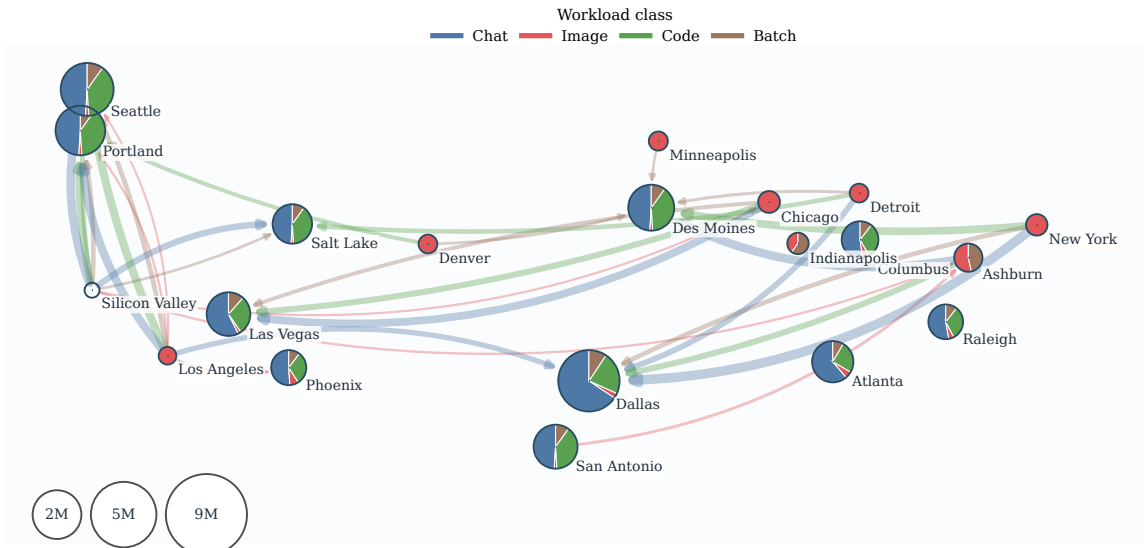


Figure 1: 20-node U.S. scale-up at demand scale 35x. Node pies show the processing mix across chat, image, code-review, and batch-training workloads, with pie size proportional to total processing. Colored curves show the largest active inter-node transfers for each workload class, with thicker curves indicating higher transferred token volume. The figure makes the merit-order geography visible: low-cost hubs in the Northwest, Midwest, and Texas absorb most chatbot traffic, while multiple workload classes share the same backbone routes.

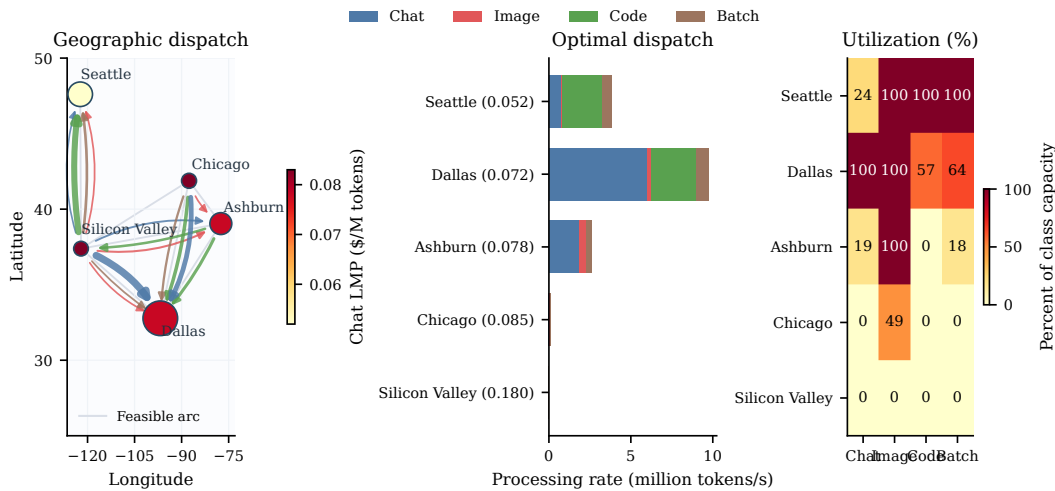


Figure 2: 5-node market outcome at demand scale 35x. Left: geographic dispatch map with node size proportional to total processing and active flows drawn between metros and colored by workload class. Center: optimal processing by node and workload class; parenthesized node labels report electricity prices in \$/kWh. Right: class-specific utilization rates. Cheap nodes carry most of the system load, while image generation and code-review capacity become locally scarce.

rises from \$41.9/M tokens to \$89.2/M tokens, while the number of scarce node-class pairs grows from four to five. This is the same qualitative behavior observed in many electricity markets near peak load, where prices remain moderate until a binding capacity margin disappears, and then the marginal price rises sharply.

The congestion pattern emerges earlier than the price cliff. The first congested link appears by scale 10x, but system cost and image prices remain fairly smooth until image-generation capacity becomes tight across most of the network. This distinction is operationally important, as a planner can observe congestion well before

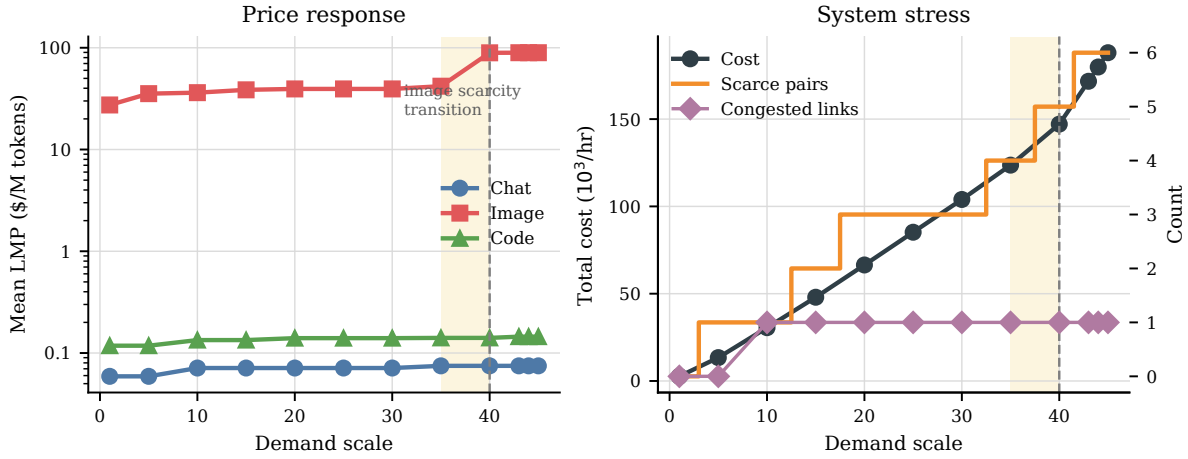


Figure 3: Market dynamics under demand growth in the 5-node network. Left: mean locational prices by workload class in \$/M tokens. Right: total operating cost, scarce node–class pairs, and congested links. The most pronounced transition occurs in image generation between scales 35× and 40×; the log price axis compresses the visual jump.

Table 4: Nested formulation comparison at the 5-node, 35× operating point. Mean prices are reported in \$/M tokens.

Model	Cost/hr	Chat	Image	Congestion
Baseline LP	\$123,635	0.0748	41.90	1
Transfer-aware LP	\$127,007	0.0770	38.90	4
Congestion-QP variant	\$123,635	0.0748	41.90	1
Uniform Opex adder	\$163,140	0.3186	47.99	1

the market reaches the more severe regime in which small demand increases generate large price changes.

4.3 Transfer-aware and latency-aware models reveal hidden bottlenecks

Table 4 treats the main variants as nested abstractions rather than unrelated algorithms. The transfer-aware model in (10) changes the economic interpretation of the network constraints in a substantive way. Using the baseline LP formulation, the 5-node system reports one congested token-equivalent link and a cost of \$123,635/hr. Under the transfer-aware LP, cost rises to \$127,007/hr with four links saturate physically. The difference is driven almost entirely by image generation, whose bytes-per-token ratio is large enough to consume entire backbone links even when the useful token flow looks modest.

Latency constraints change prices even more sharply. Tightening the chatbot latency requirement from 100 ms to 15 ms and the code-review limit from 200 ms to 20 ms partitions the 5-node network into an eastern cluster (Ashburn, Dallas, Chicago) and a western cluster (Silicon Valley, Seattle). While overall cost increase is modest at only 0.29%, the local price impact shows dramatic changes: Silicon Valley’s chatbot price rises from \$0.083/M tokens to \$0.180/M tokens with a 117% increase, due to a fact that it can no longer export latency-sensitive demand to cheaper eastern nodes.

Note that adding the uniform non-energy Opex adder used in the extended-cost experiment increases total cost from \$123,635/hr to \$163,140/hr in a 31.95% increase, but leaves the optimal dispatch unchanged because the adder shifts all nodes in parallel. This contrast reveals a useful insight that heterogeneous transfer and latency effects change allocations, whereas uniform accounting adders mostly change the price level.

4.4 Scale-up and settlement

The same qualitative patterns persist in the 20-node network. At demand scale 35×, the baseline model clears 43.89 million tokens/s at \$353,702/hr with 28 scarce node–class pairs. Dispatch again follows electricity merit order that cheap hubs such as Seattle, Portland, Des Moines, and Dallas are heavily utilized, while expensive California nodes are displaced for chatbot traffic and only re-enter when image-generation capacity becomes scarce. Figure 1 makes the spatial pattern visible. Chatbot service concentrates in the Pacific Northwest, Mountain West, Midwest, and Texas, while image-generation utilization is close to 100% at most sites. The 20-node system becomes infeasible at scale 40×, indicating that aggregate image-generation capacity, not just local congestion, becomes the dominant system bottleneck.

Notet that the settlement implied by the dual prices is revenue adequate in the 5-node baseline case. Aggregate user payments are \$139,446/hr, compute providers receive \$137,613/hr, network providers receive \$1,784/hr, and the residual merchandising surplus is \$49.71/hr. This calculation should be read as an accounting interpretation of the dual variables, not as an independent empirical validation. Its value is to show how payments split across compute, transfer, and residual congestion revenue under a nodal service-price settlement. Tracking how the surplus changes with demand and congestion is a natural extension for realistic market considerations.

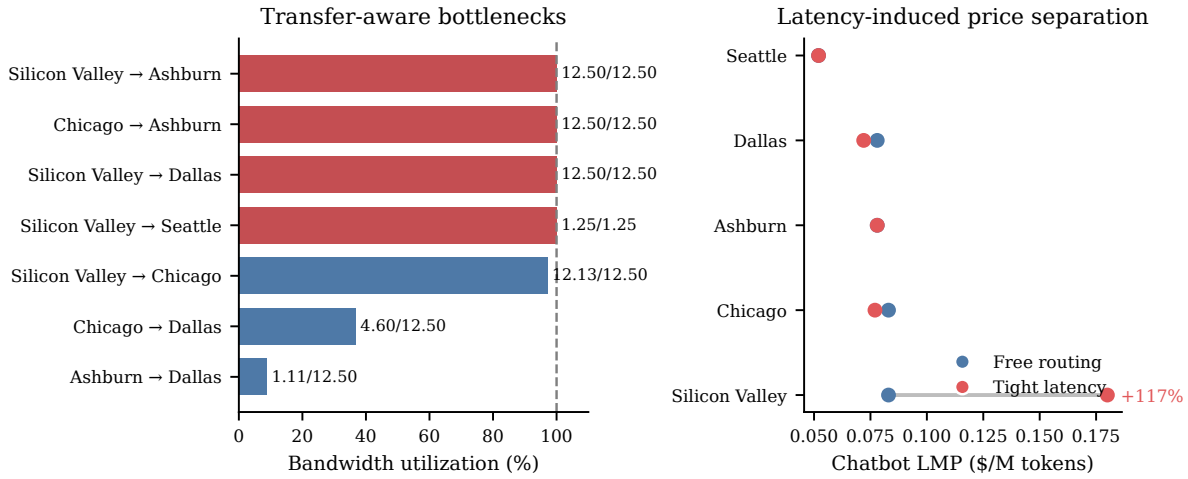


Figure 4: Left: physical bandwidth utilization of active links under the transfer-aware LP with four links fully saturated. Right: chatbot locational prices in \$/M tokens before and after imposing tight latency limits. The largest increase occurs at Silicon Valley, which becomes partially isolated from cheaper eastern supply.

5 Discussion

The authors would like to emphasize that the proposed framework should be read as a model of an emerging infrastructure market rather than as a precise description of today’s API business. Current providers still compete primarily on capability, latency, and ecosystem, and many pricing decisions are strategic rather than marginal-cost based in this emerging sector with (nearly) sustaining capital inflows. That is typical of an early-growth sector. The value of the present formulation is to identify the pricing objects that become important once adoption broadens, infrastructure utilization tightens, and return on geographically distributed assets becomes an operational concern.

The model is especially useful in a heterogeneous fleet. Different accelerators, hardware vintages, and service classes imply different throughput, energy intensity, transfer demand, and latency feasibility. That is exactly why older hardware (such as Nvidia A100, H100) can remain valuable for lower-priority or batch services even after it ceases to be competitive for frontier interactive workloads. A market that exposes nodal compute scarcity and transfer scarcity can therefore improve short-run dispatch efficiency and, eventually, provide clearer signals for specialization, interconnection, and asset-mix decisions.

The results should therefore not be reduced to the simple rule “put data centers where electricity is cheap.” Low electricity price is the first-order merit-order driver, but it is not sufficient for the fact that transfer-heavy workloads can saturate links, and latency-sensitive workloads may require nearby capacity even when local electricity is expensive. Remote low-cost regions are naturally valuable for delay-tolerant or data-light workloads; expensive urban or coastal capacity can still have option value for interactive services; and interconnection investment has a measurable shadow value through link congestion rents. Consumer-facing prices also need not expose raw locational volatility like wholesale electricity prices. Longer-term contracts, subscriptions, or two-part tariffs

could smooth marginal service costs in the same spirit as retail electricity contracts. The point is that the underlying marginal prices are still important for operational control and investment decisions, even if they are not directly visible to end users.

Lastly, the formulation is intentionally stylized. It is static, deterministic, and continuous. And it does not represent queueing dynamics, discrete accelerator allocation, reliability constraints, carbon accounting, or privacy restrictions on data movement. It also treats the power system as exogenous, whereas in practice the AI service infrastructure and electricity system are coupled through data-center load. These simplifications matter if the goal is operational deployment. They are less problematic if the goal is to identify the right marginal pricing objects. For that purpose, the model isolates the essential economics cleanly, where energy cost determines the baseline merit order, compute scarcity adds nodal rents, and data transport adds location-specific congestion rents that depend on workload characteristics. Our ongoing work extends the framework to multi-period demand uncertainty, explicit investment decisions, hardware retirement and repurposing, and joint optimization with the underlying power grid.

6 Conclusion

We presented a network-constrained token-flow market for distributed GenAI services on geographically distributed AI service infrastructure. The model yields locational marginal service prices that decompose into energy, scarcity, and transfer components, while the transfer-aware extension prices network usage in physical data units.

The numerical study shows that the prices identify merit-order dispatch, expose capacity cliffs, reveal bandwidth bottlenecks, and quantify the regional market segmentation created by tight latency requirements. This suggests that locational pricing is a useful design principle for an emerging AI service infrastructure in which

heterogeneous workloads and heterogeneous assets must be coordinated rather than treated as an undifferentiated cloud resource. If GenAI continues to diffuse into daily life and work, such pricing mechanisms are likely to become more important, not less, for both operational control and the design of future competitive markets.

Acknowledgement

Shaohui Liu is partially supported by the MIT Energy Initiative Future Energy System Center. The experiments are partially supported by U.S. National Science Foundation ACCESS and NAIRR programs. The authors thank Dr. Shen Wang, Dr. Audun Botterud, and the anonymous reviewers for their constructive feedback and suggestions. The authors acknowledge the use of ChatGPT and Claude to assist in the writing and editing of this manuscript. The authors reviewed and approved all content for accuracy and originality.

References

- [1] Ravindra K. Ahuja, Thomas L. Magnanti, and James B. Orlin. 2001. Minimum Cost Flow Problem. In *Encyclopedia of Optimization*. Springer US, 1382–1392. doi:10.1007/0-306-48332-7_283
- [2] Ross Baldick. 2018. Locational Marginal Pricing. Course notes for EE394V: Restructured Electricity Markets: Locational Marginal Pricing. <https://users.ece.utexas.edu/~baldick/classes/394V/Locational.pdf> Accessed 2026-03-16.
- [3] Cynthia Barnhart, Niranjan Krishnan, and Pamela H. Vance. 2008. Multicommodity Flow Problems. In *Encyclopedia of Optimization*. Springer US, 2354–2362. doi:10.1007/978-0-387-74759-0_407
- [4] Stephen P. Bradley, Arnoldo C. Hax, and Thomas L. Magnanti. 1977. Network Models. In *Applied Mathematical Programming*. Addison-Wesley, Chapter 8. <https://web.mit.edu/15.053/www/AMP-Chapter-08.pdf> MIT-hosted PDF version, accessed 2026-03-16.
- [5] California Independent System Operator. 2010. Appendix C: Locational Marginal Price. https://www.aiso.com/documents/appendicesc-f-fifthereplacementcaiso/tariff_15-dec-10.pdf Fifth replacement electronic tariff, effective December 15, 2010.
- [6] Data Center Map. 2026. Data Center Map: USA. <https://www.datacentermap.com/usa/> ; manually curated and accessed 2026-03-27.
- [7] Deloitte. 2026. The State of AI in the Enterprise - 2026 AI Report. <https://www.deloitte.com/cz-sk/en/issues/generative-ai/state-of-ai-in-enterprise.html> Accessed 2026-04-05.
- [8] Anish Devasia. 2025. Data Center Operating Costs: Complete Guide (2026). The Network Installers. <https://thenetworkinstallers.com/blog/data-center-operating-costs/> Accessed 2026-03-16.
- [9] Digital China Summit. 2024. National Supercomputing Internet Platform Builds a “Highway” for Digital China. <https://www.digitalchina.gov.cn/magazine/4/25/technology/1867.html> Translated title; article on the Digital China Summit website, accessed 2026-03-16.
- [10] Stephen Frank and Steffen Rebennack. 2016. An Introduction to Optimal Power Flow: Theory, Formulation, and Examples. *IEEE Transactions* 48, 12 (2016), 1172–1197. doi:10.1080/0740817X.2016.1189626
- [11] IAEI Magazine. 2026. How Much Electricity Does a Data Center Use? Complete 2025 Analysis. <https://iaeimagazine.org/electrical-fundamentals/how-much-electricity-does-a-data-center-use-complete-2025-analysis/> Page updated 2026-01-01; accessed 2026-03-16.
- [12] F. P. Kelly, A. K. Maulloo, and D. K. H. Tan. 1998. Rate Control for Communication Networks: Shadow Prices, Proportional Fairness and Stability. *Journal of the Operational Research Society* 49, 3 (1998), 237–252. doi:10.1057/palgrave.jors.2600523
- [13] Steven H. Low and David E. Lapsley. 1999. Optimization Flow Control—I: Basic Algorithm and Convergence. *IEEE/ACM Transactions on Networking* 7, 6 (1999), 861–874. doi:10.1109/90.811451
- [14] Ministry of Industry and Information Technology of the People’s Republic of China. 2025. Notice on Issuing the Action Plan for Computing Power Interconnection. https://www.miit.gov.cn/zwgk/zcwj/wjfb/tz/art/2025/art_1bbbd7e75dc4f48b75d6d2109f2e9ab.html Document No. Gong Xin Bu Xin Guan [2025] 119, accessed 2026-03-16.
- [15] Ministry of Industry and Information Technology of the PRC. 2026. MIIT Advances the “1+M+N” National Computing Power Interconnection Node System. https://www.miit.gov.cn/jgsj/xgj/gzdt/art/2026/art_0df3c73645a64d7dab09f8246acf7049.html , accessed 2026-03-16.
- [16] Daniel P. Palomar and Mung Chiang. 2006. A Tutorial on Decomposition Methods for Network Utility Maximization. *IEEE Journal on Selected Areas in Communications* 24, 8 (2006), 1439–1451. doi:10.1109/JSAC.2006.879350
- [17] Fred C. Schweppe, Michael C. Caramanis, Richard D. Tabors, and Roger E. Bohn. 1988. *Spot Pricing of Electricity*. Springer US. https://books.google.com/books/about/Spot_Pricing_of_Electricity.html?id=Sg5zRPWrZ_gC
- [18] Yosef Sheffi. 1984. *Urban Transportation Networks: Equilibrium Analysis with Mathematical Programming Methods*. Prentice-Hall, Englewood Cliffs, NJ. https://books.google.com/books/about/Urban_Transportation_Networks.html?id=zx1PAAAAMAAJ
- [19] Stanford Institute for Human-Centered Artificial Intelligence. 2025. Economy | The 2025 AI Index Report. <https://hai.stanford.edu/ai-index/2025-ai-index-report/economy> Accessed 2026-04-05.
- [20] Steven Stoft. 2002. *Power System Economics: Designing Markets for Electricity*. Wiley. https://books.google.com/books/about/Power_System_Economics.html?id=DrTEsqJRKrYC
- [21] U.S. Energy Information Administration. 2026. Electricity Open Data Browser: Retail Sales by State and Sector. <https://www.eia.gov/opendata/index.php/browser/electricity/retail-sales> ; accessed 2026-03-27.